Energy scales of the doped Anderson lattice model

Hanhim Kang
Department of Chemistry, Pohang University of Science and Technology, Pohang 37673, Korea

Kristjan Haule, Gabriel Kotliar, and Piers Coleman
Department of Physics and Astronomy, Rutgers University, New Jersey 08854, USA

Ji-Hoon Shim
Department of Chemistry, Pohang University of Science and Technology, Pohang 37673, Korea
and Department of Physics, Pohang University of Science and Technology, Pohang 37673, Korea

(Received 7 August 2018; published 12 April 2019)

This paper explores the energy scales of the doped Anderson lattice model using dynamical mean-field theory (DMFT), using a continuous-time quantum Monte Carlo (CTQMC) impurity solver. We show that the low temperature properties of the lattice cannot be scaled using the single ion local Kondo temperature T_K but instead are governed by a doping-dependent coherence temperature T^* which can be used to scale the temperature dependence of the spectral function, transport properties, and entropy. At half-filling T^* closely approximates the single ion T_K, but as the filling n_c is reduced to zero, T^* also vanishes. The coherence temperature T^* is shown to play a role of effective impurity Kondo temperature in the lattice model, and physical observables show significant evolution at T^*. In the DMFT framework we showed that the hybridization strength of the effective impurity model is qualitatively affected by the doping level, and determines T^* in the lattice model.

DOI: 10.1103/PhysRevB.99.165115

I. INTRODUCTION

The Kondo effect was first observed as a resistivity minimum in dilute magnetic alloys [1]. Kondo accounted for the resistivity minimum as a consequence of an antiferromagnetic superexchange between the magnetic impurity and conduction electrons [2]. This antiferromagnetic coupling was later revealed to be a relevant coupling, renormalizing to strong coupling at a characteristic energy scale called the Kondo temperature [3–6]. Based on a strong-coupling expansion, Nozières showed that the ground state of a magnetically screened Kondo impurity is described by a local Fermi liquid [7]. After that, a slave-particle mean-field theory showed that Kondo physics can be understood as the residue of a symmetry-breaking transition that occurs in the large N limit of the spin degeneracy, in which the Kondo temperature plays the role of a critical temperature for the phase transition [8,9].

In a large class of f-electron intermetallic materials called "heavy electron" compounds, such as the family of 115 compounds, CeMIn$_5$ (M=Co,Rh,Ir), the localized f electrons form a periodic lattice of magnetic moments whose low energy physics is described by a Kondo lattice model [10]. A generic phase diagram of the Kondo lattice was proposed by Doniach [11], who argued that if the Kondo coupling is weak the magnetic Rudermann-Kittel-Kasuya-Yosida (RKKY) interaction overcomes the formation of Kondo singlets, giving rise to an ordered magnetic ground state [10,12,13]. This state has a small Fermi surface because only the conduction electrons contribute to the charge transport. However, if the Kondo coupling is strong, it gives rise to a paramagnetic ground state which resembles the Nozières Fermi liquid state of the Kondo impurity model. Such "heavy Fermi liquids" (HFL) display carrier effective masses up to $\sim 10^3$ times larger than in conventional metals. In the HFL state, the localized moments bind to electrons, forming composite f quasiparticles which hybridize with the conduction sea, giving rise to an enlarged Fermi surface of heavy quasiparticles.

One of the long-standing questions concerns how the HFL phase evolves upon raising the temperature, and in particular, whether additional scales, beyond the single-ion Kondo temperature, are required to describe the gradual loss of coherence in the HFL [14–18]. Theoretically, the slave-boson approach showed that an additional low energy Fermi-liquid energy scale ($T_{\rm FL}$) develops in HFL [19]. Later numerical studies using the dynamical mean-field theory (DMFT) confirmed that this Fermi-liquid energy scale exists, identifying it as the temperature at which resistivity develops a maximum [20]. However, there is still no final consensus between these different studies on the precise relationship between the coherence temperature scale and the evolution of the large Fermi surface [19–22]. These considerations motivate an integrated study of thermodynamic, transport, and spectroscopic properties of the Kondo lattice model, with the goal of connecting experimental, analytic, and numerical studies.

In this article we report on a detailed study of Anderson lattice model in the Kondo lattice regime using DMFT [23–26], with a continuous-time quantum Monte Carlo (CTQMC) impurity solver [27]. The study varied the hybridization strength, temperature, and the doping level to cover a wide range of the phase diagram and investigate the scaling properties. Maximum-entropy methods were used to analytically continue from imaginary to real time to obtain dynamical spectral functions [28,29].

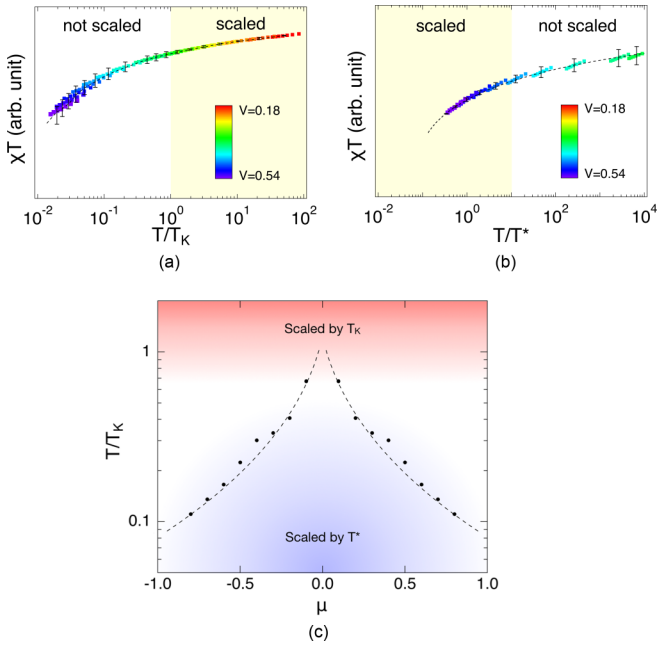

FIG. 1. Local static spin susceptibility of the Anderson lattice model scaled (a) by T_K and (b) by T^*, computed at chemical potential $\mu = -0.8$, for a range of hybridization between $V = 0.18$ (red) and $V = 0.54$ (purple). The dashed lines are the best fit and the error bars show the mismatch between the best-fit line and actual data. (c) Schematic phase diagram showing the variation of T^* with chemical potential, and the regions where the data scales with T_K (red) and with T^* (blue). The dashed line is a guide to the eye.

II. MODEL HAMILTONIAN

The single-orbital Anderson lattice model is written as

$$H = \sum_{i\sigma} \epsilon_f f^\dagger_{i\sigma} f_{i\sigma} + U \sum_i n^f_{i\uparrow} n^f_{i\downarrow} - t \sum_{\langle ij\rangle\sigma} (c^\dagger_{i\sigma} c_{j\sigma} + \text{H.c.}) + V \sum_{i\sigma} (c^\dagger_{i\sigma} f_{i\sigma} + \text{H.c.}) - \mu \sum_{i\sigma} \left(n^f_{i\sigma} + n^c_{i\sigma}\right), \quad (1)$$

where $f^\dagger_{i\sigma}$ ($f_{i\sigma}$) is a creation (annihilation) operator of the f electron with spin σ at site i, $c^\dagger_{i\sigma}$ ($c_{i\sigma}$) is a creation (annihilation) operator of the conduction electron with spin σ at site i, and $n^\alpha_{i\sigma} = \alpha^\dagger_{i\sigma}\alpha_{i\sigma}$ ($\alpha = f, c$).

For convenience, all energy scales are written in units of D, the half-bandwidth of the conduction band, and the Boltzmann constant k_B is set to unity. We considered a two-dimensional square lattice with half-bandwidth $D = 4t$. To achieve the Kondo lattice regime, we place the f level at the bottom of the band, choosing $\epsilon_f = -1.0$ and $U = 2.0$, so that the energy of the doubly occupied state $\epsilon_f + U = 1.0$ lies at the top of band. The hybridization V, chemical potential μ, and inverse temperature β were varied from 0.18 to 0.54, -0.8 to 0.8, and 80.00 to 200.00, respectively.

III. SCALING BEHAVIOR

Figure 1(a) shows the local spin susceptibility $\chi_{\text{loc}}(\omega = 0)$ for $\mu = -0.8$, for a variety of hybridization values V, scaled by the single-impurity Kondo temperature T_K evaluated with the same parameters, defined by

$$T_K = \sqrt{2J_K\rho}\exp\left[-\frac{1}{2J_K\rho}\right], \quad (2)$$

where ρ is the density of states per spin of the conduction band at the Fermi level and $J_K = (|\epsilon_f - \mu|^{-1} + |\epsilon_f - \mu + U|^{-1})V^2$ is the Kondo exchange [30]. Because the undoped model ($\mu = 0.0$) is particle-hole symmetric, electron and hole doped cases behave identically [31]. The scaling collapse of the susceptibility curves at high temperatures $\chi_{\text{loc}}(T) \sim \frac{1}{T} f(T/T_K)$ shows that the high temperature physics of the Anderson lattice model is scaled by the single-ion Kondo temperature, regardless of the doping level [31], implying that the high temperature physics at $T > T_K$ is that of a single impurity model.

However the local susceptibility [Fig. 1(a)] does not scale with the single-ion Kondo temperature at low temperatures. To scale the low-T regime, we define a coherence temperature T^*, parametrized as

$$T^* = \sqrt{2J^{\text{latt}}\rho}\exp\left[-\frac{1}{2J^{\text{latt}}\rho}\right], \quad (3)$$

where $J^{\text{latt}} = jJ_K$ is an effective Kondo lattice exchange strength. The unique fitting parameter j is adjusted at each doping level to collapse the low temperature susceptibilities onto a single curve [31]. Figure 1(b) shows that the low-T susceptibilities are successfully scaled by T^* with $j = 0.3$. The emergence of the temperature scale T^* indicates that the Kondo lattice model behaves differently in the fundamental level at low-T regime.

Figure 1(c) shows how T^* varies as the chemical potential is changed. When n_c is close to 0, T^* is suppressed towards zero while when n_c is close to half-filling, T^* tends towards the single-ion Kondo temperature T_K, a result that agrees with previous studies [20].

Figure 2(a) shows the calculated momentum- and energy-resolved total spectral function

$$A(\vec{k}, \omega) = \frac{1}{\pi}\text{Im}[G_f(\vec{k}, \omega - i\delta) + G_c(\vec{k}, \omega - i\delta)] \quad (4)$$

at $\mu = -0.5$ case. At high temperatures, only the coherent conduction band is observed near the Fermi level. Lowering the temperature, an incoherent f-electron spectrum develops at the Fermi level as a sign of Kondo singlet formation. It is notable that the spectral function starts to change far above the local Kondo temperature. It agrees well with recent ARPES measurement on the Ce-115 heavy fermion compound [21,32]. Crossing through T_K, the spectra near the Fermi level becomes incoherent, and the velocity of the ill-defined quasiparticles gets smaller as the f electron develops near the Fermi energy. The spectrum is maximally incoherent at $T = T^*$, and the quasiparticle band only re-establishes its coherence below T^*.

Figure 2(b) shows the evolution of the Fermi surface. Starting from a coherent small Fermi surface at high temperatures, it continuously evolves into an incoherent large Fermi surface, which sharpens well below the coherence temperature T^*. This continuous, but nonmonotonic evolution of the Fermi surface gives a hint for nature of the non-Fermi liquid phase observed in the quantum critical region.

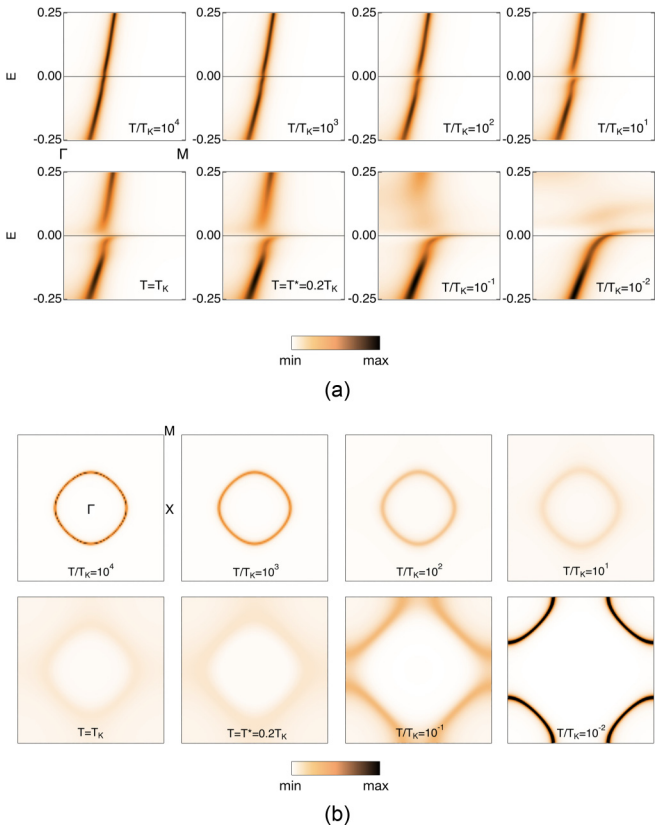

FIG. 2. Intensity plots showing the momentum and energy resolved conduction electron spectral function (a) as a function of momentum and (b) at fixed $E = 0$, showing the evolution of the Fermi surface with temperature, for $\mu = -0.5$.

Figure 3 shows the area of the Fermi surface [Figs. 3(a) and 3(b)] and imaginary part of the T matrix ($T = V^2 G_f$) of the conduction band at the Fermi level [Figs. 3(c) and 3(d)] scaled by T_K and T^*. Even though T_K scales the high-T behavior of both observables, there is no significant feature in both observables at $T = T_K$. For example, the small Fermi surface of the $\mu = -0.8$ case does not evolve to the large Fermi surface phase until far below $T = T_K$. In contrast, both Fermi surface area and the f-electron DOS at the Fermi level evolve rapidly around $T = T^*$, regardless of the chemical potential. The coherence temperature T^* also plays a significant role in the transport properties. Figure 4 shows the resistivity of $\mu = -0.2, -0.5, -0.8$ cases. In the high-T regime, the temperature dependence of the resistivity at different hybridization strengths can be scaled with the local Kondo temperature T_K as Fig. 4(a). As the temperature is reduced, the resistivity reaches a maximum and decreases forming a coherent HFL state. Figure 4(b) shows that the low-T resistivity is scaled by the coherence temperature T^*. In addition, the calculated resistivity develops its maximum value at temperatures $T \sim T^*$ which lie below the single ion T_K. This suggests that experimentally observed resistivity maxima are related to T^* and can be used to estimate this quantity.

To investigate the screening of the local moments more directly, we also calculated the entropy of the impurity degree of freedom S. In Figs. 4(c) and 4(d) the high temperature entropy approaches $\ln 2$ per site, corresponding to the

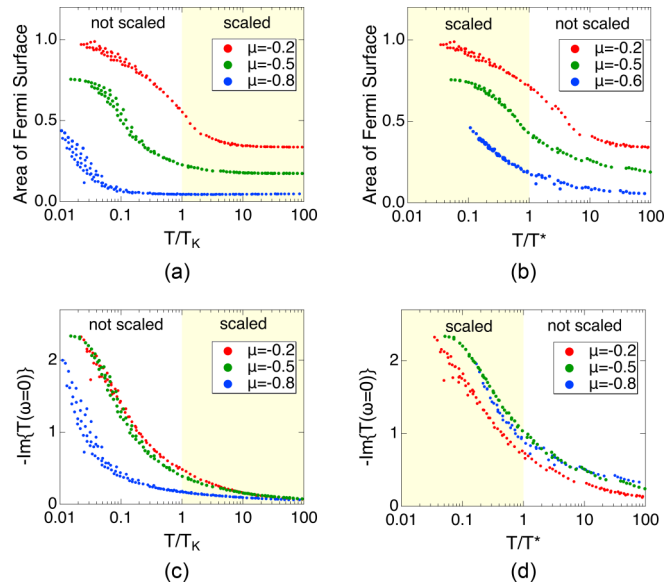

FIG. 3. Area of the Fermi surface (a) and (b) and imaginary part of the T matrix of the conduction electrons at the Fermi level (c) and (d) scaled by T_K and T^*.

unscreened local moments of the f electrons. It is remarkable that the entropy remains of order $\sim \ln 2$ even at $T < T_K$ in the heavily doped case ($\mu = -0.8$) in Fig. 4(c), indicating that the local moments are largely unscreened around $T = T_K$. Instead, as shown in Fig. 4(d), the entropy starts to drop around $T = T^*$ regardless of the doping level, although the amount of suppressed entropy depends on the doping level. The difference in the amount of suppressed entropy derives from the conduction electron occupancy n_c. Previous studies of the strong-coupling limit of the Kondo lattice model suggest that an entropy of order $n_c \ln(2)$ is lost on passing through the Kondo temperature T_K [33]. However, our results show that the suppression of magnetic entropy $S_M \sim n_c \ln(2)$ occurs at temperatures around T^*, rather than T_K. T^* thus sets the

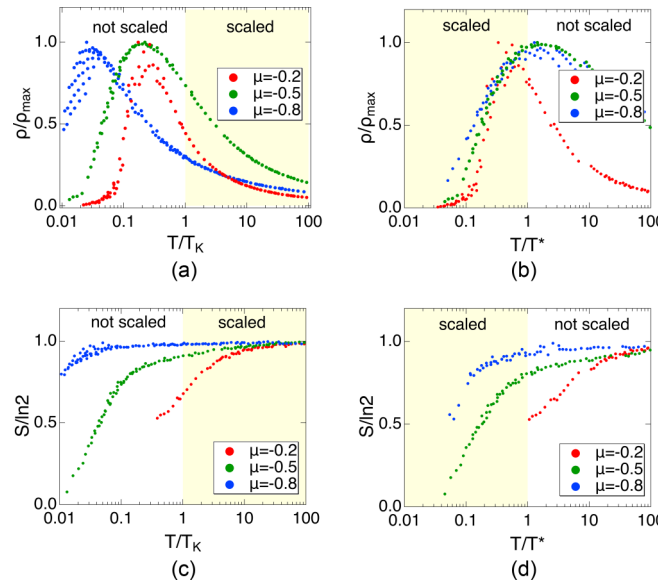

FIG. 4. Resistivity (a) and (b) and entropy (c) and (d) scaled by T_K and T^*.

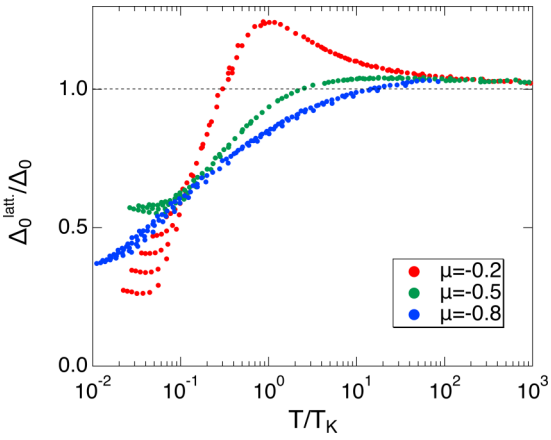

FIG. 5. Ratio between effective hybridization strength of the lattice model (Δ_0^{latt}) and hybridization strength of the impurity model.

characteristic scale at which the moments become entangled with the conduction sea in the lattice.

In the DMFT framework, the Anderson lattice is treated as an effective impurity embedded in cavity with a self-consistently determined conduction electron bath. Figure 5 shows the self-consistent hybridization strength $\Delta_0^{\text{latt.}} \equiv \text{Im}\Delta^{\text{eff.}}(z=0)$, normalized by the bare hybridization strength of the model $\Delta_0 \equiv \text{Im}\Delta(z=0)$. In the lightly doped cases ($\mu = -0.2$), the effective hybridization function is enhanced at intermediate temperatures, but regardless of doping, as the temperature decreases, the effective hybridization strength is significantly suppressed. This is due to the formation of a pseudogap structure in the cavity electronic density of states. As the pseudogap structure arises, the bath electron density of states at the Fermi level ρ decreases. This reduces the coupling constant $J_K\rho$ and the effective lattice Kondo coupling J^{latt} which determines the coherence scale

$$T^* = \sqrt{2J^{\text{latt}}\rho}\exp\left[-\frac{1}{2J^{\text{latt}}\rho}\right], \tag{5}$$

becomes smaller as a result.

IV. CONCLUSION

In conclusion, we have studied the temperature scales of the doped Anderson lattice model using single-site dynamical mean-field theory. The local Kondo temperature T_K defined by the Kondo exchange coupling J_K governs the high-temperature regime, but a new scale T^*, defined by a modified Kondo lattice exchange coupling $J^{\text{latt.}}$, governs the low-T regime. T^* has clear doping dependency, and it approaches zero as n_c goes to zero, but tends to the single-ion T_K as n_c approaches half-filling. Various physical observables such as spectral function and transport properties are scaled by T_K at high-T regime, and T^* at low-T regime.

We have also confirmed that most observables show a significant change at T^*, which is always significantly smaller than T_K. The DMFT self-consistency determines the suppression and magnitude of T^*.

ACKNOWLEDGMENTS

This research was supported by Basic Science Research Program through the National Research Foundation of Korea (NRF) funded by the Ministry of Education (2017R1D1A1B03032069), and by DOE Basic Energy Sciences Grant DE-FG02-99ER45790 (P.C.).

[1] W. J. De Haas, J. De Boer, and G. J. van dën Berg, Physica **1**, 1115 (1934).
[2] J. Kondo, Prog. Theor. Phys. **32**, 37 (1964).
[3] P. W. Anderson, J. Phys. C **3**, 2436 (1970).
[4] K. G. Wilson, Rev. Mod. Phys. **47**, 773 (1975).
[5] K. Wilson, Phys. Rep. **12**, 75 (1974).
[6] K. G. Wilson, Phys. Rev. B **4**, 3174 (1971).
[7] P. Nozières, J. Low Temp. Phys. **17**, 31 (1974).
[8] N. Read and D. M. Newns, J. Phys. C **16**, L1055 (1983).
[9] P. Coleman, Phys. Rev. B **35**, 5072 (1987).
[10] T. Kasuya, Prog. Theor. Phys. **16**, 45 (1956).
[11] S. Doniach, Physica B+C **91**, 231 (1977).
[12] M. A. Ruderman and C. Kittel, Phys. Rev. **96**, 99 (1954).
[13] K. Yosida, Phys. Rev. **106**, 893 (1957).
[14] R. Settai, T. Takeuchi, and Y. Ōnuki, J. Phys. Soc. Jpn. **76**, 051003 (2007).
[15] A. C. Hewson, *The Kondo Problem to Heavy Fermions* (Cambridge University Press, Cambridge, 1997).
[16] M. W. McElfresh, M. B. Maple, J. O. Willis, Z. Fisk, J. L. Smith, and J. D. Thompson, Phys. Rev. B **42**, 6062 (1990).
[17] J. D. Thompson and Z. Fisk, Phys. Rev. B **31**, 389 (1985).
[18] G. R. Stewart, Rev. Mod. Phys. **56**, 755 (1984).
[19] S. Burdin and V. Zlatić, Phys. Rev. B **79**, 115139 (2009).
[20] D. Tanasković, K. Haule, G. Kotliar, and V. Dobrosavljević, Phys. Rev. B **84**, 115105 (2011).
[21] Q. Y. Chen, D. F. Xu, X. H. Niu, J. Jiang, R. Peng, H. C. Xu, C. H. P. Wen, Z. F. Ding, K. Huang, L. Shu *et al.*, Phys. Rev. B **96**, 045107 (2017).
[22] K. Kummer, S. Patil, A. Chikina, M. Güttler, M. Höppner, A. Generalov, S. Danzenbächer, S. Seiro, A. Hannaske, C. Krellner *et al.*, Phys. Rev. X **5**, 011028 (2015).
[23] A. Georges, G. Kotliar, W. Krauth, and M. J. Rozenberg, Rev. Mod. Phys. **68**, 13 (1996).
[24] A. Georges and G. Kotliar, Phys. Rev. B **45**, 6479 (1992).
[25] D. Vollhardt, Phys. B: Condens. Matter **169**, 277 (1991).
[26] W. Metzner and D. Vollhardt, Phys. Rev. Lett. **62**, 324 (1989).
[27] P. Werner, A. Comanac, L. de' Medici, M. Troyer, and A. J. Millis, Phys. Rev. Lett. **97**, 076405 (2006).
[28] R. K. Bryan, Eur. Biophys. J. **18**, 165 (1990).
[29] M. Jarrell and J. E. Gubernatis, Phys. Rep. **269**, 133 (1996).
[30] J. R. Schrieffer and P. A. Wolff, Phys. Rev. **149**, 491 (1966).
[31] See Supplemental Material at http://link.aps.org/supplemental/10.1103/PhysRevB.99.165115 for the scaling behavior of the local spin susceptibility of the Anderson lattice model with various chemical potentials.
[32] S. Jang, J. D. Denlinger, J. W. Allen, V. S. Zapf, M. B. Maple, J. N. Kim, B. G. Jang, and J. H. Shim, arXiv:1704.08247.
[33] C. Lacroix, Solid State Commun. **54**, 991 (1985).